INFLUENCE OF NON-ISOTROPIC DIFFUSION ON EFFECTIVE REACTION RATES IN CATALYST PARTICLES

M. J. TAULAMET†‡, O. M. MARTÍNEZ†‡, G. F. BARRETO†‡ and N. J. MARIANI†‡

† *Departamento de Ingeniería Química, Facultad de Ingeniería, UNLP, La Plata,*
‡ *Centro de Investigación y Desarrollo en Ciencias Aplicadas "Dr. J. J. Ronco" (CINDECA) CONICET- CIC - UNLP, calle 47 No. 257, CP B1900AJK, La Plata, Argentina*
javier.mariani@ing.unlp.edu.ar

***Abstract*— The non-isotropic diffusion and reaction problem in cylindrical particles of different cross-sections is analyzed in this contribution employing the one-dimensional Generalized Cylinder Model (1D-GCΓ). Such a model presents a single parameter of straightforward calculation from the geometrical magnitudes of the catalyst particles. Different but uniform values of axial and transversal effective diffusivities are assumed. The performance of the 1D-GCΓ model for the effectiveness factor estimation is assessed for a variety of particle shapes and a set of kinetic expressions. Maximum errors in the predictions, varying a Thiele modulus and the axial-to-transversal diffusivities ratio, are below 6% for the first order reaction and rise up to around of 9% and 11% for a LHHW (Langmuir-Hinshelwood-Hougen-Watson) expression at the verge of the appearance of multiple steady states, in the case of Raschig rings and solid circular cylinders, respectively.**

***Keywords*— effective reaction rates, one dimensional model, reaction and anisotropic diffusion**

I. INTRODUCTION

Molding is a key step in the manufacturing process of catalyst and supports (Rosseau *et al*., 2022). The shape and the size of the particles should promote catalytic activity, facilitate mass transport through the catalyst bed and minimize pressure drop. Besides, the particle resistance to crushing and abrasion should be strengthened. The choice of the shape and size is mainly driven by the type of reactor (*e.g.* for fixed bed units, relatively large particles of several millimetres are employed to avoid high pressure drop). Among the different techniques, extrusion is the most economical and commonly used one. Special shapes as trilobes, Raschig rings, hollow cylinders, etc. can be obtained using proper dies. On the contrary, the pressed pellet catalysts (such as tablets) are prepared by compressing a dry powder (Hagen, 2015).

Diffusion and reaction in porous catalysts has been a subject of intense investigation from an experimental point of view (Haynes, 1988). Particularly, anisotropy effects can be found in pellets and extrudates due to the manufacturing process (Satterfield, 1970; Rigby and Gladden, 1998). To reduce this effect, binders and lubricants are frequently added to the pastes (Hagen, 1995).

In general, it is accepted that in extrudates the transversal effective diffusivities are smaller than the axial ones, while the opposite holds for pressed pellets. However, there is not a complete agreement on the magnitude of such an effect in the literature. According to Wijngaarden *et al*. (1998), anisotropy has not been greatly studied, but it is expected that the ratio between effective diffusivities (*i.e.*, axial-to-transversal) may be as high as 10, provided that cracks arise in the longitudinal direction of the particles due to the manufacturing process. Satterfield (1970) studied the diffusion in the axial direction of cylindrical particles and came to the conclusion that pellets prepared in the laboratory, under one-sided compression in unlubricated dies, show strong anisotropy effects. Differences in effective diffusivity, by a factor as high as 3 to 4, appeared depending on the axial position (Satterfield and Saraf, 1965; Cadle and Satterfield, 1968a). In contrast, such an effect was absent in catalysts manufactured by two-sided compression inside lubricated dies (Cadle and Satterfield. 1968b, Gibilaro and Waldram, 1981). However, Davidová and Schneider (1990) found large differences between the mean pore radius for radial and axial directions (up to 4 times), even when they employed commercialized Raschig rings manufactured by two-sided compacting process in presence of lubricants. Rigby *et al*. (1996) also reported values of the radial diffusivities that are twofold higher than the axial ones for tableted pellets.

In spite of the fact that the anisotropic diffusion and reaction in catalytic particles should be taken into account in the conservation balances (Wijngaarden *et al*., 1998) just a few specific articles on the subject can be found in the open literature. Asif *et al.* (2004, 2017) presented infinite series to approximate the effectiveness factor for the solid circular cylinders and Raschig rings undergoing non-isotropic diffusion and a first-order irreversible reaction. The authors developed such series from the particular solutions of one-dimensional problems for isotropic diffusion (*i.e.*, an infinite cylinder and a disk). A dimensionless parameter (γ) depending on axial-to-radial effective diffusivity and height-to-diameter ratios is introduced to account for anisotropic effects. The series obtained as a correction of the infinite cylinder particular solution is especially suitable when the radial diffusivity is greater than the axial one. On the contrary, the series achieved by a correction of the disk solution presents higher precision when the radial diffusivity is lower than the axial one. Maximum errors arise at $\gamma \approx 1$ (*i.e.*, radial and axial diffusivities are of the same order of magnitude for a cylindrical particle of the same height as diameter)

for the solid circular cylinder series approximation, while in the case of the Raschig ring they are reached at $\gamma \approx 0.5$.

Considering the most challenging cases as γ concerns (*i.e.*, those values that lead to the maximum errors), at least 5 terms of any of the two series are required to achieve an error below of 1% when $\Phi \approx 5$ for the solid circular cylinder (Asif *et al*., 2004) and when $\Phi \approx 10$ for the Raschig ring (Asif *et al*., 2017). However, if Φ is further increased from the above indicated values (up to around 10 for the solid circular cylinder and 15 for the Raschig ring) at least 10 terms must be used to keep such a level of precision. It is clear that the higher the Thiele modulus (Φ) the greater the number of series terms needed to keep a given level of precision. In summary, the series approximations proposed by Asif *et al*. (2004, 2017) can be considered as appropriate, but they are restricted for just two catalyst geometries (solid circular cylinders and Raschig rings) undergoing first-order irreversible reaction. In addition, a moderate effort for implementation is required.

In this context, the purpose of the present contribution is to evaluate the performance of the Generalized Cylinder Model (1D-GCΓ) (Mariani *et al*., 2008) to predict effectiveness factor for anisotropic diffusion in cylindrical particles with arbitrary cross-sections. A set of kinetic expressions, from the classical first order reaction to a more challenging LHHW case, is considered for the evaluations. The 1D-GCΓ model has a single parameter of straightforward calculation from the geometrical magnitudes of the particles. It is also stressed that an analytic expression for 1D-GCΓ model is available for a first order reaction.

II. PROBLEM STATEMENT AND 1D MODEL FORMULATION

A. Catalytic behaviour of an actual particle with non-isotropic diffusion

For the purpose of the present contribution, we will consider a single isothermal reaction within a cylindrical particle of arbitrary cross-section presenting uniform catalytic activity. The height, lateral area and volume of the cylinder are $H_a{}^o$, $S_{lat,a}$, $V_{p,a}$. The transport of species is expressed by means of the Fick law with uniform diffusion coefficients, but different in the transversal and axial directions (D_A and $D_{A,z}$, respectively for species A). Thus, the steady state conservation equations for a key-species A inside the catalytic particle in terms of transversal (x, y) and axial (z_a) coordinates are

$$D_A\left(\frac{\partial^2 C_A}{\partial x^2}+\frac{\partial^2 C_A}{\partial y^2}\right)+D_{A,z}\frac{\partial^2 C_A}{\partial z_a^2}=r_A, \quad (1a)$$

$$C_A = C_{AS} \text{ on } S_{lat,a} \text{ and at } z_a = 0,\ z_a = H_a \quad (1b)$$

where r_A is the consumption rate of A, the suffix "S" stands for the values at the external surface accessible to species, the lateral surface $S_{lat,a}$ and the bases at $z_a = 0$, $z_a = H_a$. In a general case, r_A will depend on the concentration of other species, C_i, apart from C_A. Such dependencies can be considered from the stoichiometric relations between the fluxes: $C_i = C_{iS} + (D_i v_i/D_A v_A)(C_A - C_{AS})$, where v_i and v_A are stoichiometric coefficients. Note that $(D_i/D_A = D_{i,z}/D_{A,z})$.

Negligible heat and mass external transfer resistances are assumed. Then, composition, temperature and consumption rate of A can be considered as uniform on the external surface of the particle.

By defining the dimensionless concentration $Y = C_A/C_{AS}$, the dimensionless reaction rate $r = r_A/r_{AS}$, Eqs. (1) becomes

$$\left(\frac{\partial^2 Y}{\partial x^2}+\frac{\partial^2 Y}{\partial y^2}\right)+\kappa\frac{\partial^2 Y}{\partial z_a^2}=\frac{1}{\lambda^2}r(Y), \quad (2a)$$

$$Y = 1 \text{ on } S_{lat,a} \text{ and at } z_a = 0,\ z_a = H_a \quad (2b)$$

where $\kappa = D_{A,z}/D_A$ and λ is the *reaction scale* ($\lambda^2 = D_A C_{AS}/r_{AS}$).

Introducing a scaled axial coordinate $z = z_a/\kappa^{1/2}$, Eqs. (2) can be rewritten as

$$\left(\frac{\partial^2 Y}{\partial x^2}+\frac{\partial^2 Y}{\partial y^2}\right)+\kappa\frac{\partial^2 Y}{\partial z^2}=\frac{1}{\lambda^2}r(Y), \quad (3a)$$

$$Y = 1 \text{ on } S_{lat} = S_{lat,a}/\kappa^{1/2} \text{ and at } z = 0,\ z = H_a/\kappa^{1/2} \quad (3b)$$

Equations (3a, b) are the conservation equations for an equivalent isotropic cylinder with diffusivity D_A, the same cross-section as the actual anisotropic particle, but with scaled height, lateral area and volume $(H, S_{lat}, V_p) = (H_a, S_{lat,a}, V_{p,a})/\kappa^{1/2}$. The solution of Eqs. (3a,b) can be undertaken by any procedure intended for an isotropic catalytic body. Once $Y(x, y, z)$ is obtained, it follows that the solution $Y_a(x, y, z_a)$ for the actual anisotropic cylinder is $Y_a(x, y, z_a) = Y(x, y, z_a/\kappa^{1/2})$.

By introducing in Eqs. (3a,b) the dimensionless coordinates $(x', y', z') = (x, y, z)/l$, where l is the characteristic length of the equivalent isotropic cylinder, $l = V_p/S_p$ (S_p is the total access area of the equivalent cylinder):

$$\left(\frac{\partial^2 Y}{\partial x'^2}+\frac{\partial^2 Y}{\partial y'^2}\right)+\kappa\frac{\partial^2 Y}{\partial z'^2}=\Phi^2 r(Y), \quad (3c)$$

$$Y = 1 \text{ on } S_{lat}/l^2 \text{ and at } z' = H/l \quad (3d)$$

where the Thiele modulus Φ is

$$\Phi = l/\lambda, \quad (4a)$$

The effectiveness factor for the equivalent isotropic cylinder is

$$\eta = \int_{V_p} r dV_p/V_p. \quad (4b)$$

From the equivalence $Y_a(x, y, z_a) = Y(x, y, z_a/\kappa^{1/2})$ it is not difficult to conclude that the effectiveness factor of the actual anisotropic cylinder is the same as that evaluated by Eq.(4b).

B. 1D-GCΓ model

The one-dimensional Generalized Cylinder Model (1D-GCΓ) has been developed (Mariani *et al.*, 2008) to approximate the behaviour of a catalytic particle with transport in the three spatial directions by a solid body that allows mass and heat transport in a single coordinate x, $0 < x < L$. Such a body presents a variable cross-section $S(x) = S_p(x/L)^\sigma = S_p(x')^\sigma$, where $x' = x/L$ and S_p is the total external area of the modelled particle. The 1D-GCΓ model is applied here to the equivalent isotropic cylinder described in the previous section.

The 1D-GCΓmodel has two free parameters: the diffusion length L and the shape factor σ. L is evaluated by matching the volume V_p of the particle to be modelled. Hence, $L = l(\sigma + 1)$. Thus, the 1D-GCΓ model will present the same asymptotes of η as the modelled particle at very low and very high values of Φ.

The mass conservation balance according to the 1D-GCΓ model can be written as

$$(x')^{-\sigma}\left[\frac{d}{dx'}\left((x')^{\sigma}\frac{dY}{dx'}\right)\right] = (1+\sigma)^2\Phi^2 r(Y), \quad (5a)$$

$$Y = 1 \text{ at } x' = 0 \quad (5b)$$

$$dY/dx' = 0 \text{ at } x' = 1 \quad (5c)$$

where the Thiele modulus (Φ) is the same as in the modelled catalyst particle. The effectiveness factor is obtained from

$$\eta_{1D-GC\Gamma} = (1+\sigma)\int_0^1 r(Y)(x')^{\sigma}dx'. \quad (6)$$

It is worth noting that the 1D-GCΓ model exactly encompasses the classical 1D problems in a slab ($\sigma = 0$), an infinitely long circular cylinder ($\sigma = 1$) and a sphere ($\sigma = 2$). The term "generalized cylinder" to identify this model is due to the fact that the effectiveness factor for a first-order reaction can be expressed in a way extending the well-known expression for an infinitely long solid circular cylinder (Mariani *et al*., 2003):

$$\eta_{1D-GC\Gamma}(\Phi) = \frac{1}{\Phi}\frac{I_{(\sigma+1)/2}[(1+\sigma)\Phi]}{I_{(\sigma-1)/2}[(1+\sigma)\Phi]}, \quad (7)$$

where $I_t[arg]$ is the modified Bessel function of real order t.

The remaining parameter σ is obtained by matching the second order term of the expansion series of η in powers of $(1/\Phi)$ (*i.e.* applied for high reaction rates). Then,

$$\sigma = \Gamma/(1-\Gamma), \quad (8)$$

where Γ is the parameter for the equivalent isotropic cylinder that can be evaluated by (Mariani *et al*., 2008):

$$\Gamma = \frac{\Gamma_\infty + \frac{16}{\pi}l_\infty/H}{(1+2l_\infty/H)^2}, \quad (9a)$$

with

$$l = \frac{l_\infty}{1+2l_\infty/H} \quad (9b)$$

where Γ_∞ y l_∞ are the values of the parameter Γ and the effective length l when the height H of the cylinder tends to infinite, respectively.

Equation (9a) is strictly valid for a first order reaction. However, the level precision of the estimations does not change significantly when other kinetic expressions are employed. A general expression to obtain Γ is given in Keegan *et al.* (2006). Values of Γ_∞ for different cross-section shapes are displayed in Tables 1 and 2.

C. Kinetic expressions

Three types of irreversible kinetic expressions were tested: the usual reference for a first order reaction, a zero-order reaction and a Langmuir-Hinshelwood-Hougen-Watson (LHHW) expression showing abnormal behaviour (*i.e.*, kinetics which go through a maximum as reaction proceeds):

$$\text{First-order reaction: } r = Y, \quad (10a)$$

$$\text{Zero-order reaction: } r = 1, \quad (10b)$$

$$\text{LHHW: } r = 81Y/(1+8Y)^2, \quad (10c)$$

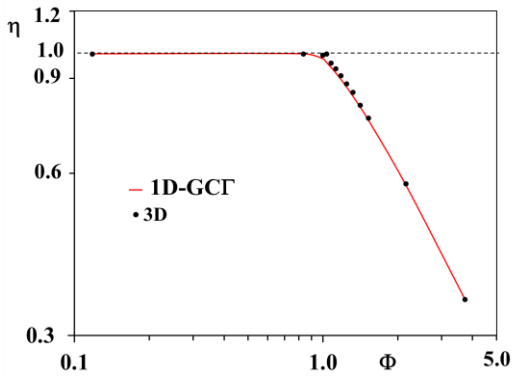

Figure 1: η vs. Φ for the actual anisotropic particle and for the 1D-GCΓ model (zero-order reaction and Raschig ring with $h = H/b = 0.25$).

Expression (10c) is particularly challenging for any approximation, as it leads close to the onset of the multiple steady-state behaviour.

III. RESULTS

The COMSOL Multiphysics® platform was used to solved Eqs. (2a,b) for the actual anisotropic cylinder or Eqs. (3a,b) for the equivalent isotropic cylinder. As expected, it was checked that the effectiveness factors η from both solutions coincide. For a given Φ, the approximate values $\eta_{1D-GC\Gamma}$ from the solution of Eqs.(5a-c) of the 1D-GCΓ model are compared with values of η on the basis of the relative error ε:

$$\varepsilon = 100(\eta_{1D-GC\Gamma} - \eta)/\eta. \quad (11)$$

As stated in section II.B, the 1D-GCΓ model was developed in such a way that it matches the asymptotes of η at very low and very high values of Φ for the actual particle. Then, the maximum deviations will appear for intermediate values of Φ. This behaviour can be observed in Fig. 1 for the zero-order kinetic (Eq. 10b) and a Raschig ring with $h = H/b = 0.25$ (see Table 1).

Maximum errors (denoted by ε_{max}) have been employed as a criterion to assess the 1D-GCΓ model precision for each kinetic expression and catalyst geometry:

$$\varepsilon_{max} = \max_{\Phi,H}|\varepsilon| \quad (12)$$

Considering the first order kinetic (Eq.10a), Table 1 shows values of ε_{max} for a variety of cross-section shapes of the cylindrical particles. In this group of particles ε_{max} arise at $\kappa \neq 0$, *i.e.*, at a finite value H given in Table 1 in dimensionless form $h = H/b$, where b is a characteristic dimension of the different cross-sections, also displayed in Table 1. It is remarked that the highest value of ε_{max} in Table 1 is 1.6%.

Table 2 shows ε_{max} for another group of cylindrical shapes, also for a first order reaction. Different behaviour from particles in Table 1 can be appreciated, as values of ε_{max} arise at $\kappa \to 0$ (*i.e.*, $h \to \infty$, dominant transversal diffusion). Besides, the highest ε_{max} in Table 2 rises to around 6%. It is noted that pellet-strings used for catalyst testing (Moonen *et al*., 2017) behave as long cylinders, $h \to \infty$.

A systematic and significant impact of the kinetic expression on the 1D-GCΓ model precision arises. As ex-

Table 1. Geometric features and ε_{max} values from the 1D-GCΓ model for different particles. First order reaction and $\kappa \neq 0$

	Particle						
	Solid circular cylinder	Raschig ring	Parallelepiped	Trilobe	Quadralobe	7-lobes central holed ring	6-notches central holed ring
Cross-section	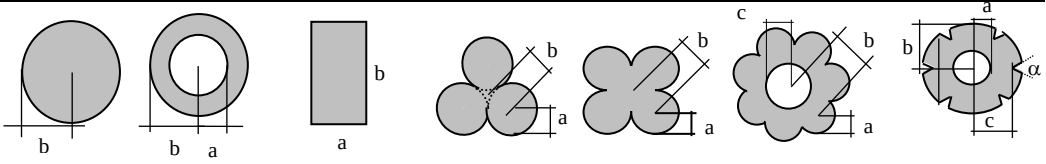						
Dimensions	b=1	a=0.5 b	a= b	a=b/1.15	a=b/1.41	a=b/2.30 c=b/0.56	a=b/2.73 c=b/0.8 α=1.047
ε_{max}	1.4%	1.3%	1.6%	1.3%	1.4%	1.1%	1.2%
h=H/b	0.35	0.20	0.20	0.43	0.35	0.22	0.07
Γ_∞	0.5	0.0	0.637	0.866	0.707	-0.375	0.222

Table 2. Geometric features and ε_{max} values from the 1D-GCΓ model for different particles. First order reaction and $\kappa \to 0$ ($h \to \infty$).

	Particle			
	8-lobes	Star	4-Holed ring	10-Holed ring
Cross-section	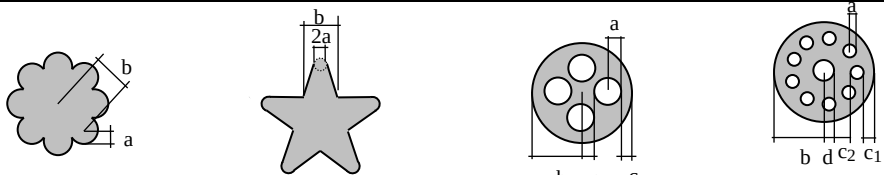			
Dimensions	a=b/2.613	a=b/3.425	a=b/2.727 c=b/3.274	a=b/8; c_1=b/5 c_2=0.3 b; d=b/4
ε_{max}	4.8%	5.3%	4.9%	5.9%
Γ_∞	0.547	0.306	-0.241	-0.636

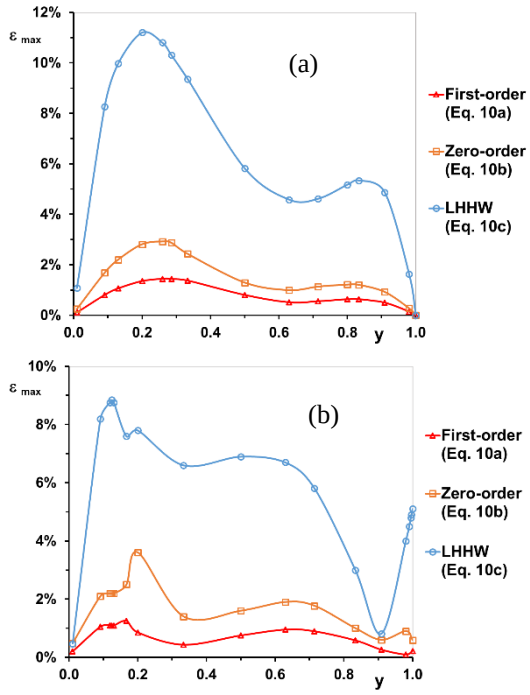

Figure 2: ε_{max} vs. $y = h/(1+h)$ for 1D-GCΓ model (a) solid circular cylinder (b) Raschig ring

pected, the highly non-linear kinetics (Eq. 10c) leads to the largest errors. Values of ε_{max} vs. $y = h/(1+h)$ employing the three kinetic expressions (Eqs. 10a-c) for the solid circular cylinder and the Raschig ring are presented in Figs. 2a and b. For the solid circular cylinder (Fig. 2a), ε_{max} occurs at an intermediate value of h in the range of 0.25-0.35 (*i.e.*, $y = 0.2 - 0.26$), with the highest value of ε_{max}= 11.2% at $y = 0.2$ for the LHHW kinetic expression (Eq. 10c). Likewise, values of ε_{max} for the Raschig rings in Fig. 2b arise for h within the range 0.1425-0.25 (*i.e.*, $y = 0.125 - 0.2$) and the highest ε_{max} is around 8.9% at $y = 0.125$, also for LHHW kinetics. In addition, the highest values of ε_{max} for the zero-order expression are consistently lower: 2.9% for the solid circular cylinder ($y = 0.26$ in Fig. 2a) and 3.6% for the Raschig ring ($y = 0.2$ in Fig. 2b).

It is important to remark that $\varepsilon_{max} \to 0$ when $y \to 1$ (*i.e.*, $\kappa \to 0$, $h \to \infty$) for the solid circular cylinder, as the 1D-GCΓ model becomes exact (irrespective of the kinetic expression) while, on the contrary, the model keeps a residual error for the Raschig ring. However, as it can be appreciated from Fig. 2b, it is considerably less than the maximum value of ε_{max} for each kinetic expression.

Although ε_{max} is a suitable indicator of the predictive capability of the 1D-GCΓ model, from a practical point of view it is of interest to assess an average error for a given range of the Thiele modulus. Then, we defined such an average error as:

$$\varepsilon_{av} = \int_{\Phi_1}^{\Phi_2} |\varepsilon| d\Phi / (\Phi_2 - \Phi_1). \qquad (13)$$

The range $0.5 < \Phi < 2.5$ was selected to include the zone of maximum errors at the intermediate values of Φ.

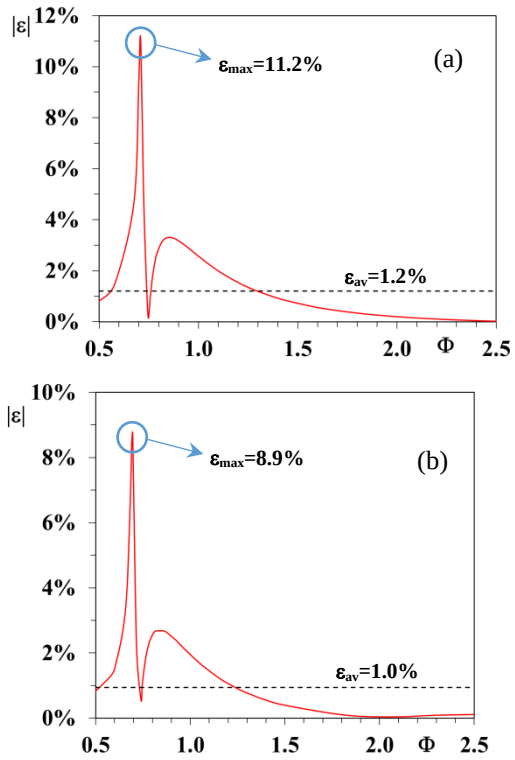

Figure 3: |ε| vs. Φ for 1D-GCΓ model and LHHW kinetic expression (Eq. 10c). (a) solid circular cylinder ($y = 0.2$) (b) Raschig ring ($y = 0.125$)

Figures (3a) and (3b) show the values of $|\varepsilon|$ vs. Φ for the solid circular cylinder ($y = 0.2$) and for the Raschig ring ($y = 0.125$), respectively, in both cases for the LHHW kinetics (Eq. 10c). Despite the fact that the values of y are those for which ε_{max} takes place, values of ε_{av} are around 1.2% and 1.0%, respectively. Therefore, it can be concluded that 1D-GCΓ model allows reaching a noticeably high level of precision on average and tolerable maximum errors, even when a highly challenging kinetic expression is employed.

IV. CONCLUSIONS

The predictive capability of the one-dimensional Generalized Cylinder Model (1D-GCΓ) to estimate the effectiveness factor in a variety of cylindrical particles with different cross-sections under anisotropic diffusion and reaction is analysed in this contribution. The axial and the transversal effective diffusivities are assumed independent of the position. Simultaneously, a set of kinetic expressions are employed that include from the elementary first order reaction to a challenging LHHW expression with parameters that lead close to the onset of the multiple steady state behaviour. The 1D-GCΓ model has a single free parameter of straightforward calculation from the shape of the catalyst particles. An advantage of the model stems on the fact that, for any particle geometry undergoing a first order reaction a simple analytical expression to obtain the effectiveness factor is available.

The performance of the model is evaluated by computing the maximum error (ε_{max}) in the effectiveness factor estimation varying the Thiele modulus and the axial-to-transversal diffusivity ratio (κ) from 0 to ∞. For a first order reaction ε_{max} was lower than 1.6% and 6% when considering groups of particles for which such values arise either at finite κ or as $\kappa \to 0$ (*i.e.*, transversal diffusivity much higher than the axial one), respectively.

Irrespective of the catalyst geometry, the more complex the kinetic expression the higher the values of ε_{max}. For the extensively used solid circular cylinders and Raschig rings with LHHW kinetics (Eq. 10c), ε_{max} rises up to around 9% and 11% (for finite values of κ), respectively. In addition, if average errors in the practically common range of Thiele modulus 0.5-2.5 are considered for such particles, values less than 1.2% arise.

If higher precision is required in the estimation of effectiveness factor, advanced 1D models (as the 1D-VD model, Mariani *et al*., 2013) can be used, although at expense of more involved parameter evaluations.

ACKNOWLEDGEMENTS

The authors are thankful for the financial support of the following Argentine Institutions: CONICET (PIP 11220200102005CO) and UNLP (PID I226). M. J. Taulamet, N. J. Mariani, O. M. Martínez and G. F. Barreto are research members of the CONICET.

REFERENCES

Asif, M. (2004) Efficient expressions for Effectiveness factor for a finite cylinder. *Chem. Eng. Res. and Des.* **82**, 605–610

Asif, M., Ibrahim A.A., Mohammed Y.A. and Al-Ghurabi E.H. (2017) Effectiveness factor of two-dimensional ring-shaped catalyst pellets. *Pol. J. Chem. Technol.* **19**, 99-105.

Cadle, P.J. and Satterfield C.N. (1968a) Anisotropic Diffusivities in Pressed Boehmite Pellets. *Ind. Eng. Chem. Fundam.* **7**, 192-197.

Cadle, P.J. and Satterfield C.N. (1968b) Uniformity of diffusivity in a nickel base steam-hydrocarbon reforming catalyst. *Ind. Eng. Chem. Fundam.* **7**, 189-192.

Davidová, H. and Schneider P. (1990) Chromatographic determination of effective diffusivities of Raschig ring-shaped catalyst: Radial anisotropy of pellets. *Applied Cat.* **66**, 167-180.

Gibilaro, L.G. and Waldram S.P. (1981) Measurement of Effective Binary Gas Diffusion Coefficients in Porous Catalysts. *J. Catal.* **67**, 392–401.

Haber, J., Block, J.H. and Delmon B. (1995) Manual of methods and procedures for catalyst characterization. *Pure & Appl. Chem.* **67**, 1257-1306.

Hagen, J. (2015) Catalyst Shapes and Production of Heterogeneous Catalysts. Chapter 6 in *Industrial Catalysis: A Practical Approach.* 3rd edition. Wiley-VCH Verlag GmbH & Co. KGaA.

Haynes, H.W. Jr. (1988) The Experimental Evaluation of Catalyst Effective Diffusivity. *Catal. Rev. - Sci. Eng.* **30**, 563-627.

Keegan, S.D., Mariani, N.J., Martínez, O.M. and Barreto G.F. (2006) Behavior of Catalytic Pellets at High

Reaction Rates. The Effect of Edges. *Ind. Eng. Chem. Res.* **45**, 85-97.

Mariani, N.J., Keegan, S.D., Martínez, O.M. and Barreto G.F. (2008) On the evaluation of effective reaction rates on commercial catalyst by means of a one-dimensional model. *Catal. Today.* **133–135**, 770–774.

Mariani, N.J., Keegan, S.D., Martínez, O.M. and Barreto, G.F. (2003) A one-dimensional equivalent model to evaluate overall reaction rates in catalytic pellets. *Trans IChemE*. **81** (A), 1-10.

Mariani, N.J, Taulamet, M. J., Keegan, S.D., Martínez, O.M. and Barreto, G.F. (2013) Prediction of effectiveness factor using one-dimensional approximations for complex pellet shapes and abnormal kinetics expressions. *Ind. Eng. Chem. Res.* **52**, 15321−15329.

Moonen, R., Alles, J., Ras, E.-J., Harvey and C., Moulijn, J.A. (2017) Performance Testing of Hydrodesulfurization Catalysts Using a Single-Pellet-String Reactor. *Chem. Eng. Technol.* **40-11**, 2025–2034.

Rigby, S.P., Cheah, K.-Y. and Gladden, L.F. (1996) NMR imaging studies of transport heterogeneity and anisotropic diffusion in porous alumina pellets. *Applied Cat. A: General.* **144**, 377-388.

Rigby, S.P. and Gladden, L.F. (1998) The Use of Magnetic Resonance Images in the Simulation of Diffusion in Porous Catalyst Support Pellets. *J. Catal.* **173**, 484–489.

Rosseau, L.R.S., Middelkoop, V., Willemsen, H.A.M., Roghair, I., van Sint Annaland, M. (2022) Review on Additive Manufacturing of Catalysts and Sorbents and the Potential for Process Intensification. *Front. in Chem. Eng.* **4**, 834547.

Satterfield, C.N. (1970) *Mass Transfer in Heterogeneous Catalysis.* MIT Press, Cambridge, MA.

Satterfield, C.N. and Saraf, S.K. (1965) Anisotropic Diffusivities in Pressed Catalyst Pellets. *Ind. Eng. Chem. Fundam.* **4**, 451-454.

Wijngaarden, R.I., Westerterp, K.R. and Kronberg, A. (1998) *Industrial Catalysis.: Optimizing Catalysts & Processes*. Wiley VCH, Weinheim.

Received: May 31, 2022
Sent to Subject Editor: August 1, 2022
Accepted: October 3, 2022
Recommended by Subject Editor Laura Briand